# Equivalent model for the phase dynamics of a metamaterial inspired patch antenna

Gianpaolo Papari and Antonello Andreone

Citation: Journal of Applied Physics **119**, 084505 (2016); doi: 10.1063/1.4942523
View online: http://dx.doi.org/10.1063/1.4942523
View Table of Contents: http://scitation.aip.org/content/aip/journal/jap/119/8?ver=pdfcov
Published by the AIP Publishing



JOURNAL OF APPLIED PHYSICS **119**, 084505 (2016)

# Equivalent model for the phase dynamics of a metamaterial inspired patch antenna

Gianpaolo Papari[1,2,a)] and Antonello Andreone[1]
[1]*Dipartimento di Fisica, Universitá di Napoli Federico II, Piazzale Tecchio 80, 80125 Napoli, Italy and CNR-SPIN, UOS Napoli, Piazzale Tecchio 80, 80125 Napoli, Italy*
[2]*IMAST S.c.a.r.l.—Technological District on Engineering of Polymeric and Composite Materials and Structures, Piazza Bovio 22, 80133 Napoli, Italy*

(Received 4 December 2015; accepted 9 February 2016; published online 26 February 2016)

We present a simple model for a patch antenna based on metamaterial concepts operating in the microwave region with a bandwidth of 1.9–2.6 GHz. The small size and the relatively large operational band make this device exploitable for electromagnetic energy harvesting in urban environments. Describing the antenna by an equivalent circuit composed of a transmission line having right/left hand properties with a *RC* load, we can properly account for the phase dynamics in correspondence of resonances characterized by a specific handedness. The model is validated measuring the response of the reflection scattering parameter $S_{1,1}$ for a copper prototype fabricated on a FR4 printed circuit board. © *2016 AIP Publishing LLC*. [http://dx.doi.org/10.1063/1.4942523]

## I. INTRODUCTION

The ongoing growth of electromagnetic sources aimed to improve cellphone/wireless communications has motivated the developments of devices capable of partial harvesting of radiating waves.[1,2] The electromagnetic energy can be naturally collected through an antenna and a rectifier and then re-directed into desired lines/loads.[3,4] For energy harvesting devices, small dimensions are required in order to allow an easy installation in different environments (indoor, streets, and open spaces).[1,4]

A useful and fruitful approach to shrink the size of a patch antenna without losing performance is to apply the concepts of metamaterial transmission lines (MMTL).[5–8] Following this approach, capacitors and inductors are properly designed (in the form of interdigital lines and meanders, respectively) and inserted into the transmission line (TL) in order to set resonant modes at wavelengths much larger than antenna transverse dimensions.[9,10] A metamaterial based TL can propagate both right handed (RH) and left handed (LH) modes depending on the concordance or discordance, respectively, between the sign of group velocity ($v_g$) and phase velocity ($v_p$).[6] Accordingly, a positive or negative refractive index $n \propto v_g \propto (\partial S_{2,1}/\partial\omega)^{-1}$ can be defined, similarly to the case of light propagation across a bulk metamaterial. Therefore, a real metamaterial-inspired antenna (MMA) is also indicated as a composite right-handed/left-handed transmission line, since its emission band is typically characterized by a mixing of RH and LH resonant modes. In recent years, the MMTL approach has been extensively applied to design and fabricate small antennas working in different bands.[7,10–16] MMAs show modes whose handedness can be addressed by studying the dispersion relation $\beta(\omega)$ obtained through the formula $\beta(\omega) = 1/a\cos^{-1}(1 + ZY/2)$, where a is the unit length, and Z and Y are the impedance and admittance of the TL, respectively. The order of resonant modes is then achieved by imposing the Bloch-Floquet periodic condition, $\beta_n = n\pi$, with $n = 0 \pm 1, \pm 2, ....$[17] The most commonly used parameter to study the performance of an antenna is the reflection scattering coefficient $S_{1,1}$, which provides access to the return loss of the device. Unfortunately, a clear relationship between $\beta(\omega)$ and the directly measured $S_{1,1}$ does not exist.

Here, we propose an electrical equivalent model useful to describe the dynamics of phase $Arg(S_{1,1})$ in a MMA. The antenna under study is a circular patch having a bandwidth large enough to harvest electromagnetic energy from network systems like UMTS (1800 MHz), GSM (2100 MHz), and WiFi/bluetooth (2400 MHz). The $S_{1,1}$ parameter presents a series of resonances whose phase dynamics follows either a left- or right-handed behaviour, in accordance with the standard properties shown by a LH/RH transmission line. Our model can properly account for the phase changes in correspondence of the main resonant modes under the simple assumption that the device equivalent circuit is given by a transmission line having right/left handed properties with a *RC* load.

## II. ANTENNA DESIGN AND PROPERTIES

Circular patch structures are ideal systems for developing wide band antennas suitable for working with different field polarisation.[18] A sketch of the proposed device is presented in Figs. 1(a) and 1(b). The radiator element, the circular patch, has been implemented with the insertion of an interdigitated capacitance. On the front side, the device presents a meander driving the signal to the patch and working as matching circuit for the antenna, usually characterised by a strong capacitive coupling (i.e., $Im(Z_{in}) < 0$).[7] On the backside of the board, an inductive ring having the same diameter of the patch has been patterned and linked to the radiating element using a via. The magnitude of the reflection parameter $S_{1,1}$ has been simulated using the commercial software *CST MICROWAVE STUDIO®*. The simulated

a)papari@fisica.unina.it

 

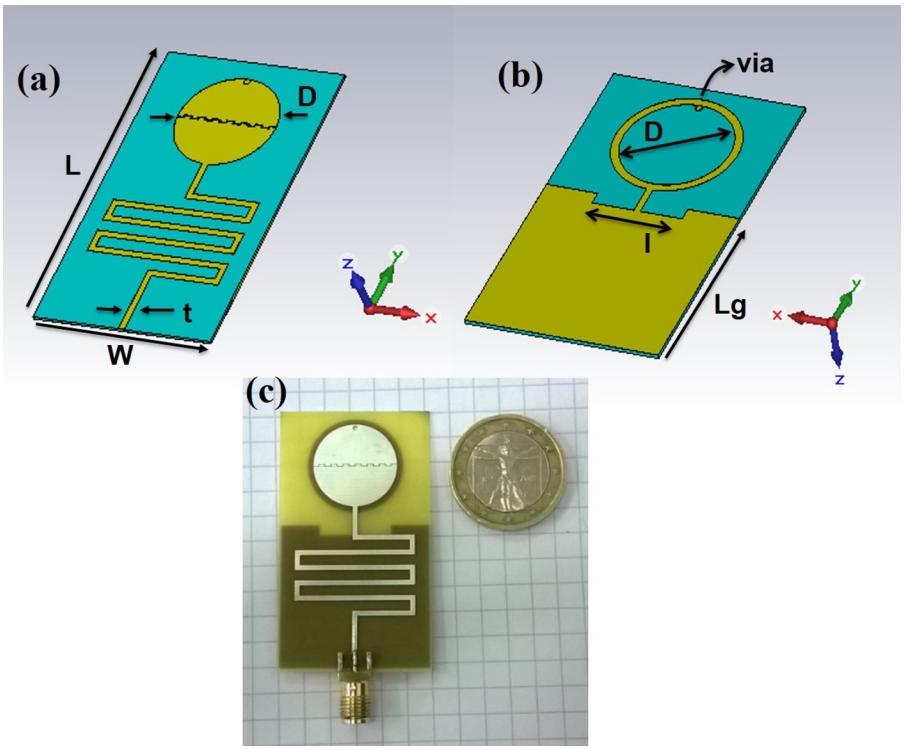


FIG. 1. Sketch of (a) the top side and (b) the backside of the MM-inspired patch antenna. (c) A picture of the antenna fabricated using 0.7 mils copper on a standard FR4 substrate (thickness 0.5 mm). Dimensions are $L = 52.0$ mm, $W = 30.0$mm, $D = 16.6$mm, $t = 1.0$mm, $Lg = 27.5$mm, and $l = 14.0$mm.

excitation signal at the port is a TEM mode, which, according to the reference system displayed in Fig. 1, can be written in terms of the time harmonic field $\vec{E}(y,t) = Re\{\vec{E}(y)e^{-i\omega t}\}$, where $\vec{E}(y) = E_z\, e^{iky}$, $\omega = 2\pi f$ is the angular frequency, $k$ is the wave vector, and $E_z$ is the modulus of the electric field along $z$. The simulated modulus of $S_{1,1}$ is displayed in Fig. 2, clearly showing the $-10$ dB bandwidth in the frequency range of 1.9–2.6 GHz.

In Fig. 3(a), the 3-D gain pattern is reported. The gain at the band frequency 2.1 GHz is about 0.9 dB. Two main lobes compose the far field radiation pattern having extension $\theta = [\pm 41.5°]$ in the azimuthal and $\phi = [\pm 43°]$ in the vertical plane (see Figs. 3(b) and 3(c), respectively). The antenna shows radiative properties aligned to the best devices having similar characteristics presented in literature.[19,20] The relatively low gain is the result of the trade-off with the large bandwidth. Performance optimisation is beyond the scope of this work; nevertheless, the pattern of the antenna can be improved at the expenses of a higher complexity in the structure or employing a lower $\tan\delta$ substrate. The results reported in Refs. 19–21 show that larger bandwidth can be acquired enhancing the number of resonating modes of the hosting TL through the insertion of additional $LC$ components, even if with a further gain reduction.

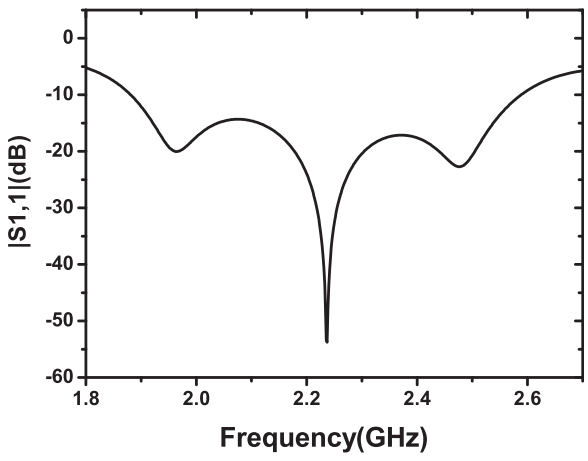


FIG. 2. Simulated reflection parameter magnitude $|S_{1,1}|$ of the metamaterial-inspired antenna as a function of frequency.

Contrarily to the case of a monopole circular antenna, presenting a wide central resonance only, the MMA shows a few resonant modes on average 0.2 GHz afar from $f_0 = c/(4\,n\,D) \approx 2$ GHz,[18] where $D$ is the patch diameter and $n = \sqrt{\epsilon_r}$ is the refractive index of the substrate, respectively. Since the higher order modes are expected at frequencies roughly multiple of $f_0$, we infer that the band extension is due to the beating between the fundamental mode and the $LC$ resonances introduced in TL through the insertion of the meander and the interdigitated capacitance.[14,20] In the following, it will be shown that in correspondence of specific resonances, the phase $Arg(S_{1,1})$ behaviour can be used to extract direct information on the signal propagation inside the metamaterial-inspired antenna, since it behaves differently if a left- or a right-handed mode is involved. Therefore, by looking at the phase dynamics and using a simple circuit model, one can successfully predict the mode handedness of the antenna.

## III. ELECTRICAL MODEL OF MMA

In order to trace out the handedness of the resonant modes excited in the device, we propose a simple model based on the idea that a MMA can be represented as the composition of single mesh RH/LH TL[6,21,22] expressed by an equivalent transmission line impedance $Z_{TL}$ and ended on

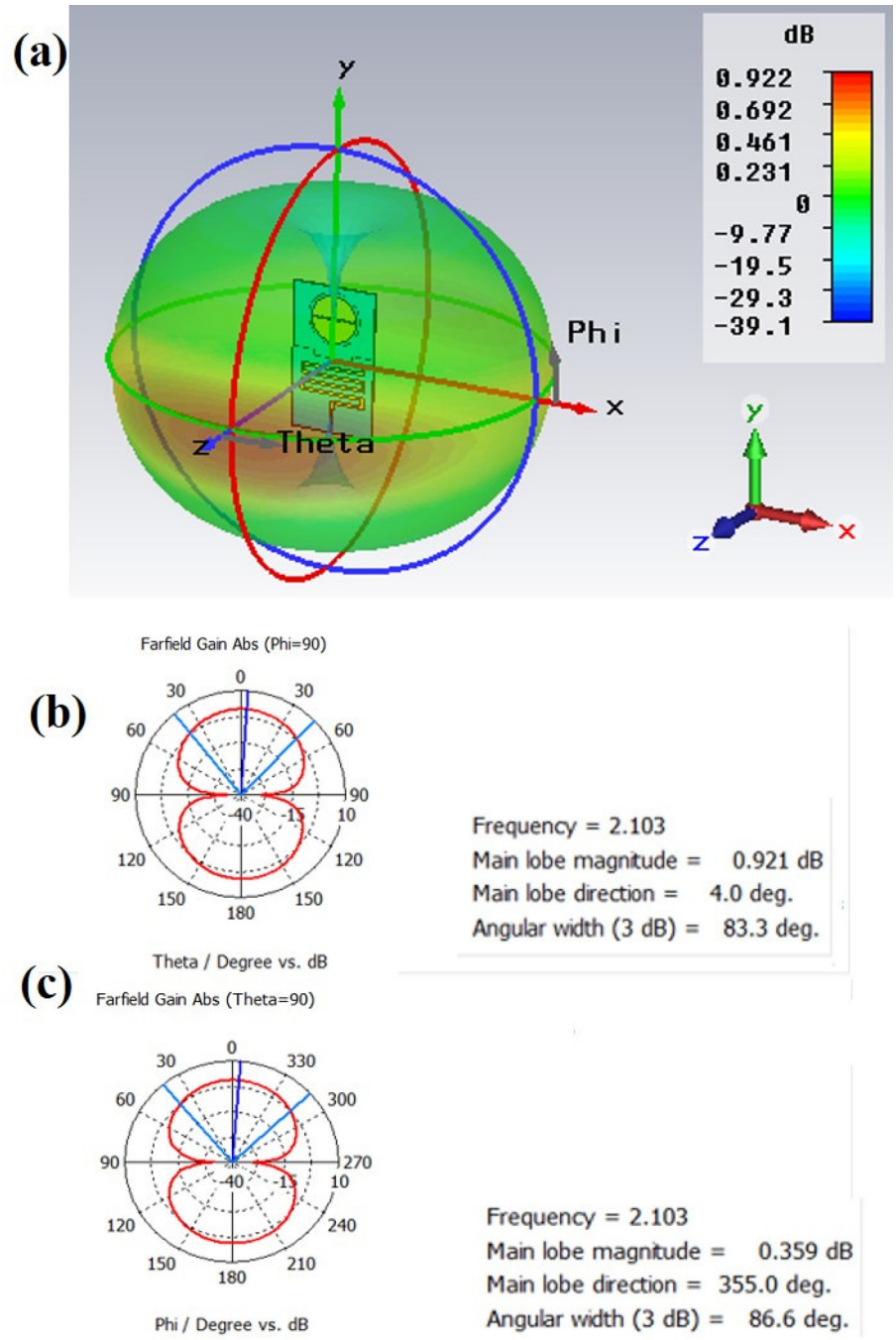


FIG. 3. (a) The computed full 3-D far field pattern at 2.1 GHz. (b) and (c) The same pattern in polar coordinates as a function of the azimuthal and elevation angle, respectively.

a *RC* load. The lumped element electrical model is presented in Fig. 4. The single MMTL mesh works as matching circuit[7] for the patch antenna represented as a parallel between a resistor and a capacitor.[23] The single RHTL mesh is a $\pi$ circuit composed of a couple of series inductors shunted through a capacitor, whereas the ($\pi$) single mesh LHTL antenna is composed of series capacitors shunted through an inductor.[6] Within the model, the impedances are defined as $Z_{L_i} = i\omega L_i$, $Z_{C_i} = 1/i\omega C_i$, and $Z_{R_i} = R_i$, where $i = r, l$ depending on the handedness of the propagating mode. By a proper choice of $L_i$, $C_i$, and $R_i$, we can calculate the input impedance $Z_{in}$ and simulate the phase dynamics of the scattering parameter $S_{1,1}$ ($S$ from now on) obtainable as $S = (Z_{in}/Z_0 - 1)/(Z_{in}/Z_0 + 1)$,[24] which in turn depends on the chosen reference impedance of the TL $Z_0 = Z_A = Z_R \| Z_C$.

According to the handedness, $Z_{in}$ can be written

$$Z_{in,r} = i\omega L_r + \frac{Z_{A,r} + i\omega L_r}{1 + i\omega Z_{A,r} C_r - \omega^2 L_r C_r} \tag{1}$$

or

$$Z_{in,l} = 1/i\omega C_l + i\omega L_l \left( \frac{1 + i\omega Z_{A,l} C_l}{1 + i\omega Z_{A,l} C_l - \omega^2 L_l C_l} \right). \tag{2}$$

The main role of $Z_A$ is to damp (through $R$) the divergence of $Z_{in}$ in correspondence of $f_{r,l} = 1/2\pi\sqrt{L_{r,l} C_{r,l}}$. $Z_{TL}$ instead provides the proper inductive coupling to the *RC* branch of the antenna for setting the resonant modes. The calculated behaviour of the magnitude and phase of $Z_{in}$ for the left- and the right-handed MMA, respectively, are

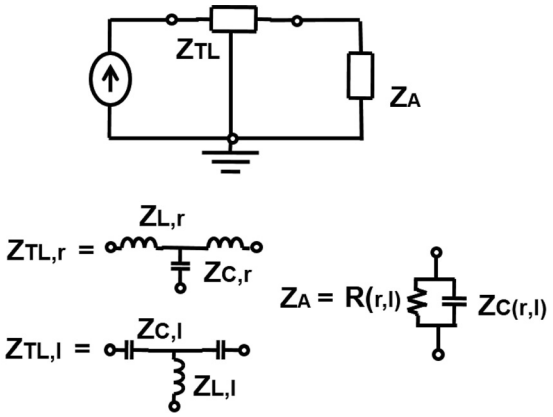


FIG. 4. Circuit model of the metamaterial-inspired antenna represented as the composition of either left-handed or right-handed transmission line applied to an *RC* circuit.

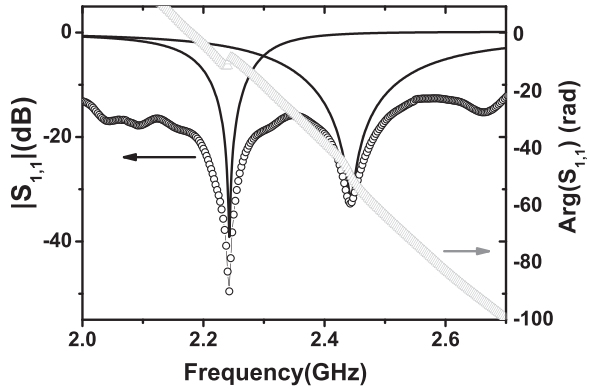


FIG. 6. The measured magnitude and phase of $S_{1,1}$ as a function of frequency are reported as dotted and triangular points, respectively. To highlight the frequency dependence, data for $Arg(S_{1,1})$ are multiplied by a factor 2. The continuous curves represent the simulated $S_{1,1}$ for the specific resonant modes $f_r$ and $f_l$.

reported in Fig. 5. We used as circuital parameters $L_l = 2.2\text{nH}, C_l = 1.0\text{pF}, R_l = 12.5\,\Omega$, and $L_r = 10.0\text{nH}, C_r = 1.0\text{pF}$, $R_r = 10.0\,\Omega$. The values for $L_{r,l}$ and $C_{r,l}$ are found by matching the resonant frequencies $f_{r,l}$, whereas the resistances $R_{r,l}$ are obtained by fitting the experimental curves of $Arg(S_{r,l})$ in correspondence of these resonances (see below). Using simple geometrical considerations, these values are roughly in agreement with what is realistically expected for the capacitance of the meander on the front board and for the inductance of the circular ring on the back side.[25–28]

Figs. 5(a) and 5(b) contain information on the magnitude of $Z_{in}$ according to the left- or right-handedness, respectively. The position of the minima (resonant modes) accounts for each frequency at which the TL reactance is zero and $Z_{in}$ substantially matches with $R$. In correspondence of the resonances, both $Arg(Z_{in,l})$ and $Arg(Z_{in,r})$ rise up, making impossible to distinguish the handedness of the resonance just by looking at the phase behaviour in correspondence of $f_{r,l}$. On the other hand, it is easy to show that only the phase of the reflection scattering parameter $S$ addresses the issue on the handedness of the modes, according to

$$S_{l/r} = (Z_{in,l/r}/Z_{A,l/r} - 1)/(Z_{in,l/r}/Z_{A,l/r} + 1). \qquad (3)$$

In particular, using the above expression, one can infer the handedness of the resonances $f_r$ and $f_l$.

## IV. SCATTERING PARAMETER MEASUREMENTS

A prototype of the antenna has been fabricated processing a 0.25 thick FR4 printed circuit board ($\epsilon_r = 4.93$, $\tan\delta = 0.021$ in the frequency range of interest) with copper 0.7 mils (about 18 $\mu$m) through galvanic and chemical processes. The outer dimensions are $W = 30\,\text{mm} \approx \lambda/5$ and $L = 52\,\text{mm} \approx \lambda/3$, where $\lambda = c/2\,\text{GHz}$ is the reference wavelength of the antenna having a bandwidth $\Delta f = (1.8 - 2.7)\,\text{GHz}$. The antenna is fed using a $50\,\Omega$ coaxial cable

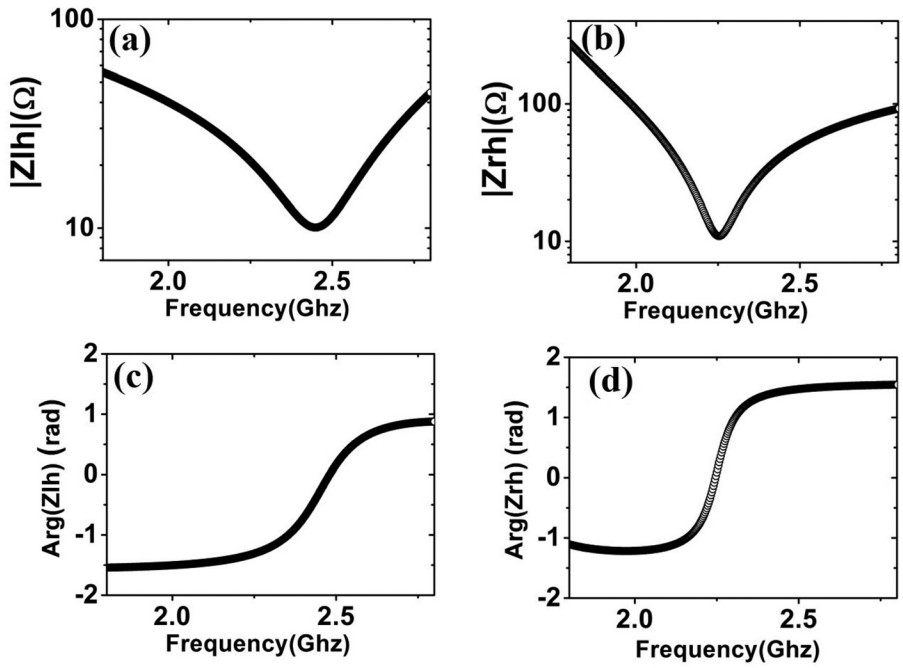


FIG. 5. (a) Magnitude and (c) phase of $Z_{in}$ for the left-handed MMA. (b) Magnitude and (d) phase of $Z_{in}$ for the right-handed MMA.

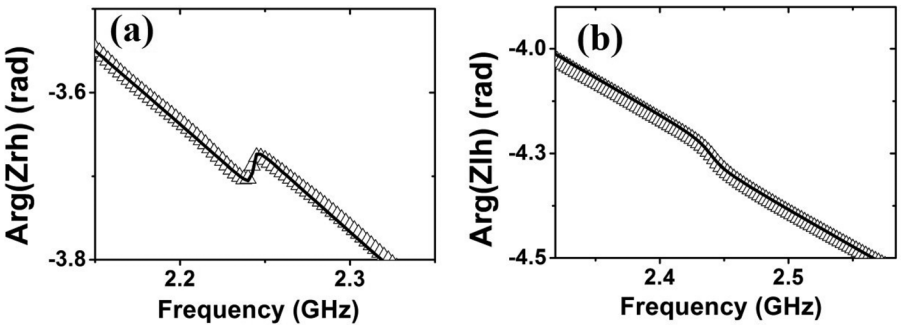


FIG. 7. Simulated (continuous line) and measured (triangular points) phase dynamics of $S_{1,1}$ near the resonance frequencies $f_r$ (a) and $f_l$ (b), respectively.

through a SMA connector (see Fig. 1(c)). The MMA presented here is the modification of a basic circular monopole patch antenna having similar performances but larger size with an effective area enclosed in a rectangle $69 \times 121\,\mathrm{mm}^2$. Hence, by applying MMTL concepts, one can reduce the total area of the antenna to more than 80%. The reflection parameter $S_{1,1}$ at the SMA port has been measured using a vectorial network analyser *HP 8720C* in the overall bandwidth. The results are reported in Fig. 6 for both magnitude and phase. One can see that experimental data for $|S_{1,1}|$ show a substantial agreement with the simulation curve reported in Fig. 2. In the same graph, the computed magnitude of the reflection scattering parameter for the LH and RH resonances (continuous lines) are also shown, indicating the estimated values of $f_l$ and $f_r$, respectively. Contrarily to the case of $Z_{in}$, $Arg(S_{l,r})$ presents a remarkable difference between the left- and the right-handed case. Specifically, the phase displays an upward (positive) turn at $f_r$ (Fig. 7(a)) and a downward (negative) turn at $f_l$ (Fig. 7(b)). Using the values found for the lumped circuital parameters, and taking also into account the delay introduced in the reflected signal by the finite extension of the antenna, in both cases, a nice matching between measurements and simulations obtained using Eq. (3) is achieved.

The standard way to assign either RH or LH characteristics to resonant modes consists into verify that[6]

$$sign(v_p) = -sign(v_g). \tag{4}$$

Therefore, the positive or negative index properties can be easily identified in correspondence of the mode labeled as $f_r$ and $f_l$ through a simple circuital model of a typical MMTL. Actually, the MMA phase evaluated in the nearness at $f_r \approx 2.25\,\mathrm{GHz}$ follows the behaviour expected from Equation (3) for a periodic LHTL, whereas the opposite happens for the $S_{1,1}$ phase dynamics at $f_l \approx 2.45\,\mathrm{GHz}$. This is not surprising because the single RH (LH) mesh (i.e., $Z_{TL,r(l)}$) behaves like a LH (RH) one when seen from the input.

## V. CONCLUSIONS

In this work, we simulated, fabricated, and measured a circular patch antenna working in the S band and whose design is inspired on the concepts of metamaterial transmission line. Because of its reduced electrical size, a single device or an array based on such radiating elements can be effectively used in a variety of different applications, like energy harvesting for wireless systems. We developed a simple but effective electrical model for the antenna that can account for $S_{1,1}$ resonance dynamics by a proper choice of the RH/LH TL $\pi$ mesh. Our finding is that positive or negative index properties (i.e., $sign(v_p) = -sign(v_g)$) can be seen by simply looking at $Arg(S_{1,1})$ behaviour close to the resonant frequencies.

## ACKNOWLEDGMENTS

We thank the company *Esseti Circuiti Stampati* for the fabrication of the antenna. The authors would like to acknowledge that part of the research activity has been conducted within the frame of the research project GREEN *PON*02 – 00029 – 2791179 granted to IMAST S.c.a.r.l. and funded by the M.I.U.R.

[1]J. W. Matiko, N. J. Grabham, S. P. Beeby, and M. J. Tudor, Meas. Sci. Technol. **25**, 012002 (2014).
[2]T. S. Almoneef and O. M. Ramahi, Appl. Phys. Lett. **106**, 153902 (2015).
[3]M. S. Jawad, N. B. Zainol, and Z. Zakaria, Microwaves RF July, 49 (2015).
[4]G. Ramesh and A. Rajan, in *2014 International Conference on Communications and Signal Processing (ICCSP)* (2014), pp. 1653–1657.
[5]C. Lin, H. Arai, and T. Suda, in *International Workshop on Antenna Technology: Small Antennas and Novel Metamaterials, iWAT* (2008), pp. 418–421.
[6]G. V. Eleftheriades, Mater. Today **12**, 30 (2009).
[7]J. Zhu and G. Eleftheriades, IEEE Antennas Wireless Propag. Lett. **8**, 295 (2009).
[8]Q. Zhao, X. Zhao, L. Kang, and Q. Zheng, Chin. Sci. Bull. **50**, 396 (2005).
[9]G. Bertin, F. Bilotti, B. Piovano, R. Vallauri, and L. Vegni, IEEE Trans. Antennas Propag. **60**, 3583 (2012).
[10]H. Mirzaei and G. Eleftheriades, IEEE Antennas Wireless Propag. Lett. **10**, 1154 (2011).
[11]H. El-Raouf, S. Zaheer, and Y. Antar, in *3rd European Conference on Antennas and Propagation, EuCAP* (2009), pp. 3572–3574.
[12]K. Agarwal, T. Mishra, M. Karim, Nasimuddin, M. Chuen, Y. X. Guo, and S. Panda, in *2013 IEEE MTT-S International Microwave Symposium Digest (IMS)* (2013), pp. 1–4.
[13]A. Erentok and R. Ziolkowski, IEEE Trans. Antennas Propag. **56**, 691 (2008).
[14]J. Liu, Y. Cheng, Y. Nie, and R. Gong, Microwaves RF November, 69 (2013).
[15]F. Herraiz-Martinez, G. Zamora, F. Paredes, F. Martin, and J. Bonache, IEEE Antennas Wireless Propag. Lett. **10**, 1528 (2011).
[16]S. Kim and J. Jang, in *2010 International Workshop on Antenna Technology (iWAT)* (2010), pp. 1–4.
[17]C. Caloz, A. Sanada, and T. Itoh, IEEE Trans. Microwave Theory Tech. **52**, 980 (2004).
[18]A. R. S. Osama Haraz, *Advancement in Microstrip Antennas with Recent Applications*, edited by A. Kishk (InTech, 2013).
[19]F. M. L. X. S. Li and D. L. Wu, in *PIERS Proceedings, Guangzhou, China, August 25–28, 2014*, p. 2478.
[20]X.-S. Li, K.-Da. Xu, D.-Y. Zhou, F. Du, and Z.-M. Liu, Microwaves RF May, 58 (2015).

[21]B. D. Bala, M. K. A. Rahim, and N. A. Murad, Microwave Opt. Technol. Lett. **57**, 252 (2015).
[22]C. Liu and K. Huang, *Metamaterial Transmission Line and its Applications, Advanced Microwave and Millimeter Wave Technologies Semiconductor Devices Circuits and Systems*, edited by M. Mukherjee (InTech, 2010).
[23]O. P. A. Hafiane and H. Assat, Electron. Lett. **39**, 1031 (2003).
[24]T. S. Bird, IEEE Antennas Propag. Mag. **51**, 166 (2009).
[25]E. B. Rosa and L. Cohen, "On the self inductance of circles," *Bulletin of the Bureau of Standards*, Vol. 4 (U.S. Government Printing Office, Washington, 1907–1908).
[26]S. Schaur and B. Jakoby, Proc. Eng. **25**, 431 (2011).
[27]M. W. den Otter, Sens., Actuators A **96**, 140 (2002).
[28]D. M. S. Goran and I. Ljiljana, Serb. J. Electr. Eng. **1**, 57 (2004).